Terahertz Sources Based on Intra-Cavity Difference-Frequency Generation in Quantum Cascade Lasers

Mikhail A. Belkin[1], Federico Capasso[1], Feng Xie[2], Alexey Belyanin[2], Deborah L. Sivco[3] Milan Fischer[4], Jérôme Faist[4], Douglas C. Oakley[5], Christopher J. Vineis[5], George W. Turner[5]

1. Harvard School of Engineering and Applied Sciences
2. Physics Department, Texas A&M University
3. Bell Laboratories
4. ETH, Zurich
5. MIT Lincoln Laboratory

ITQW, 2007

Motivation

Compact THz source

- Injection pumped
- CW at TE cooler temperature
- Widely tunable
- ~10-1000μW of CW THz power

Applications

- Spectroscopy
- Local oscillator for THz heterodyning
- Remote sensing, screening, inspection

THz QCL

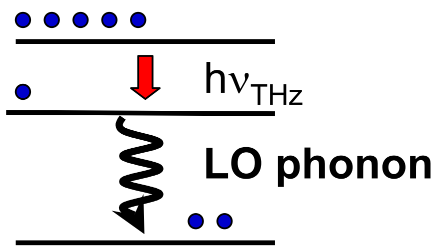

Nonradiative decay rates grow quickly with temperature in THz QCLs

T_{max} vs frequency

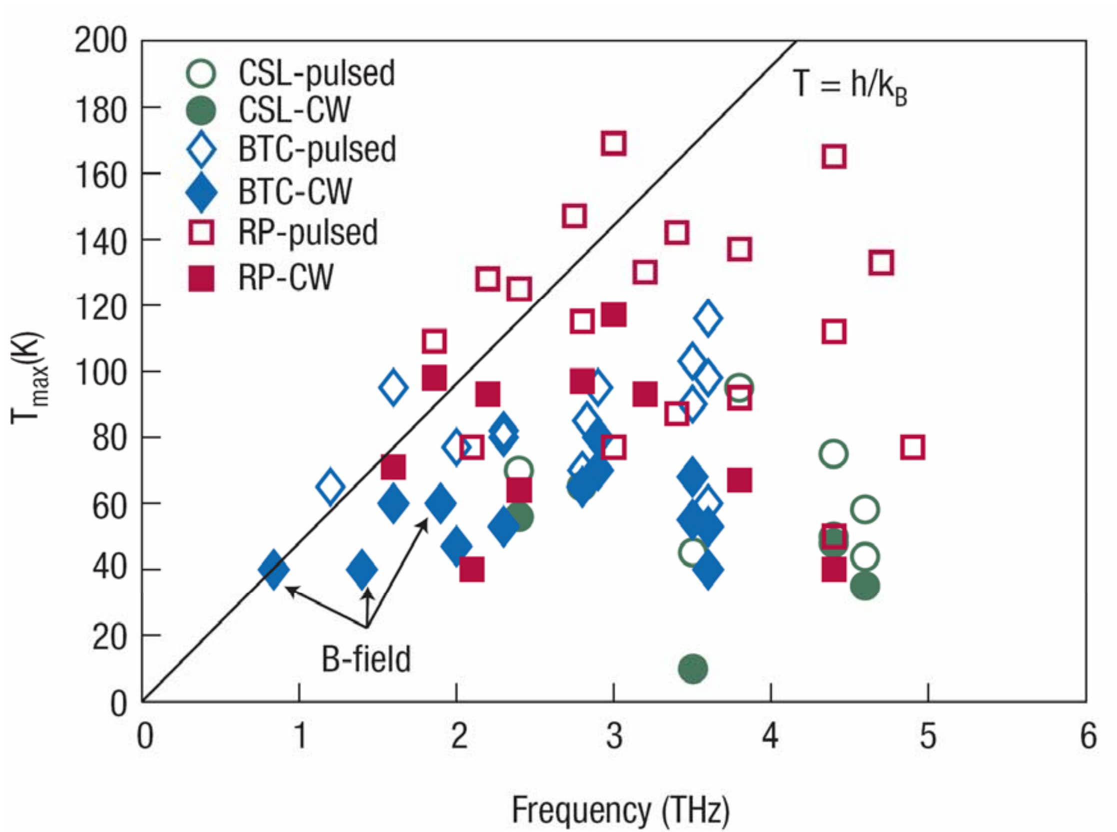

B.S. Williams, Nature Photon ***1,*** *517-525 (2007)*

Mid-IR QCL

Excellent performance in mid-infrared

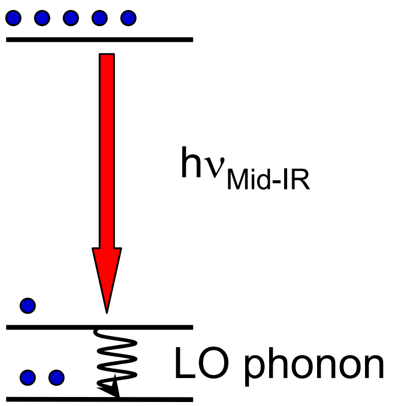

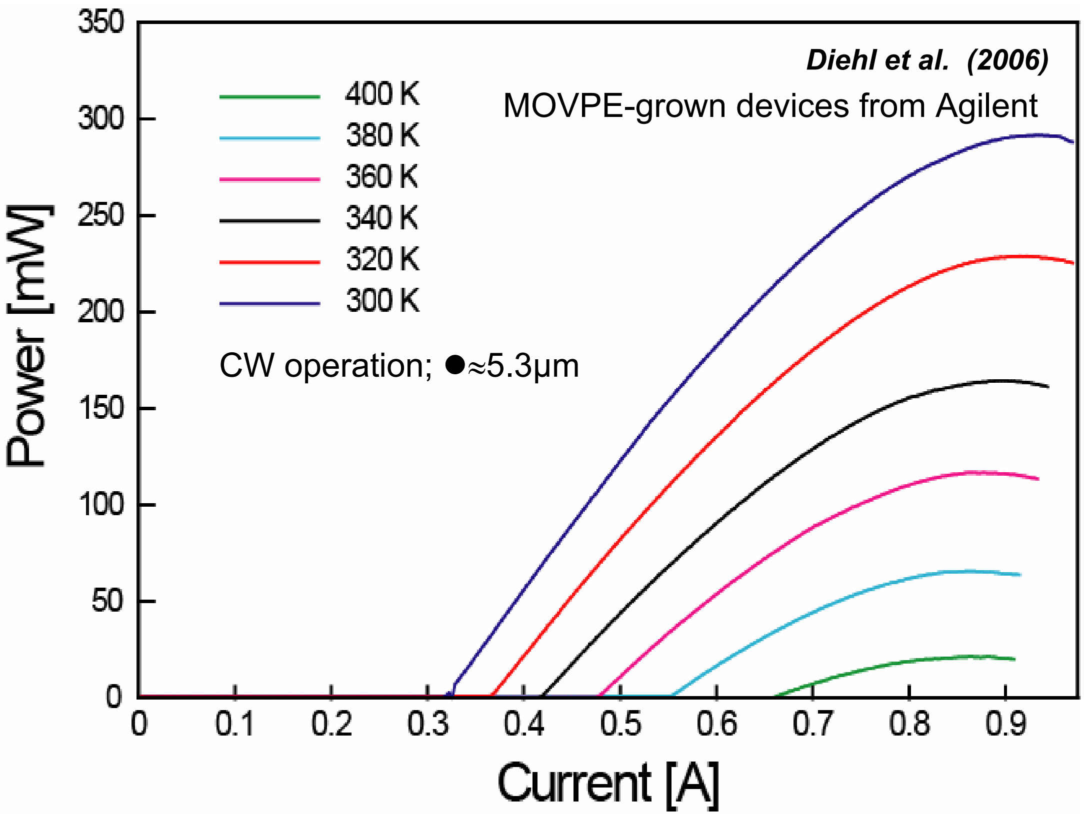

THz Difference Frequency Generation

Difference-frequency generation (DFG) occurs in a medium with second-order nonlinear susceptibility $\chi^{(2)}$

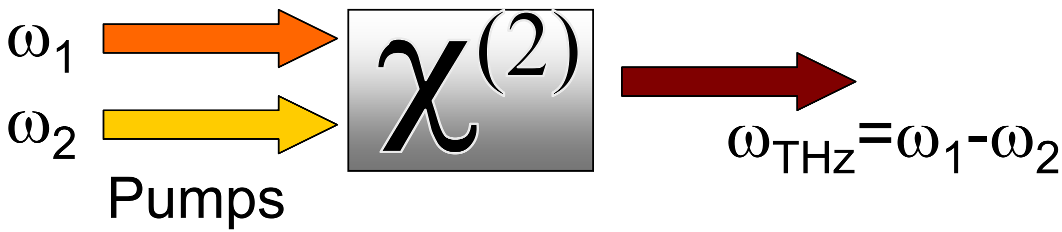

THz QCL source using intra-cavity DFG

- *Dual-frequency mid-infrared QCLs with monolithically integrated $\chi^{(2)}$.*

- *THz radiation is generated via intra-cavity DFG.*

- *Widely tunable THz source at RT (using DFB gratings for both pump lasers).*

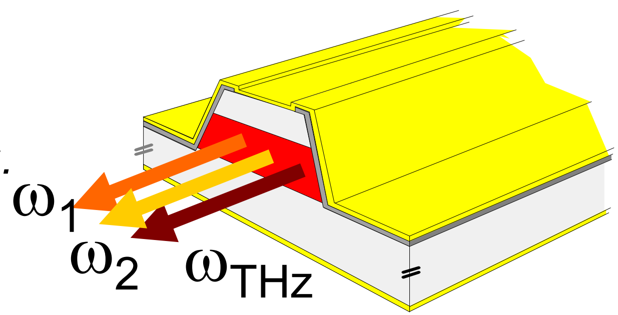

Challenges for intra-cavity THz DFG

$$I(\omega_{THz}) \propto \left|\chi^{(2)}\right|^2 I(\omega_1) I(\omega_2) \times l_{eff}^2$$

Traditional schemes for THz DFG:

Use high-intensity pumps from pulsed solid-state lasers (up to $1GW/cm^2$)

and/or

Utilize long l_{eff} (tens of mm) in transparent nonlinear crystals

Intra-cavity THz DFG in dual-wavelength mid-IR QCL:

- Relatively low pump intensities (up to $1\text{-}10MW/cm^2$)
- l_{eff} is limited by free-carrier absorption to ≏0.2mm
- Quantum well structures may have ***giant*** $\chi^{(2)}$ (up to 10^6 pm/V)

$\chi^{(2)}$ with population inversion

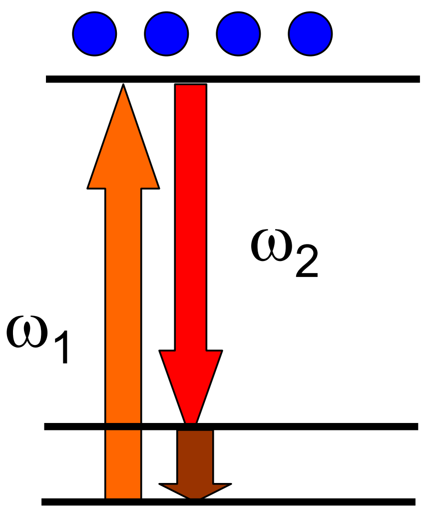

$$\chi^{(2)}(\omega=\omega_1-\omega_2)\sim\sum_{n,n'}\frac{z_{1n}z_{nn'}z_{n'1}}{(\omega-\omega_{nn'}+i\Gamma_{nn'})}\left(\frac{1}{(\omega_1+\omega_{n'1}+i\Gamma_{n'1})}+\frac{1}{(-\omega_2-\omega_{n1}+i\Gamma_{n1})}\right)$$

Quantum cascade laser structure with giant $\chi^{(2)}$.

- *Giant $\chi(2)$ with population inversion*
- *Laser action instead of absorption*

Active region design

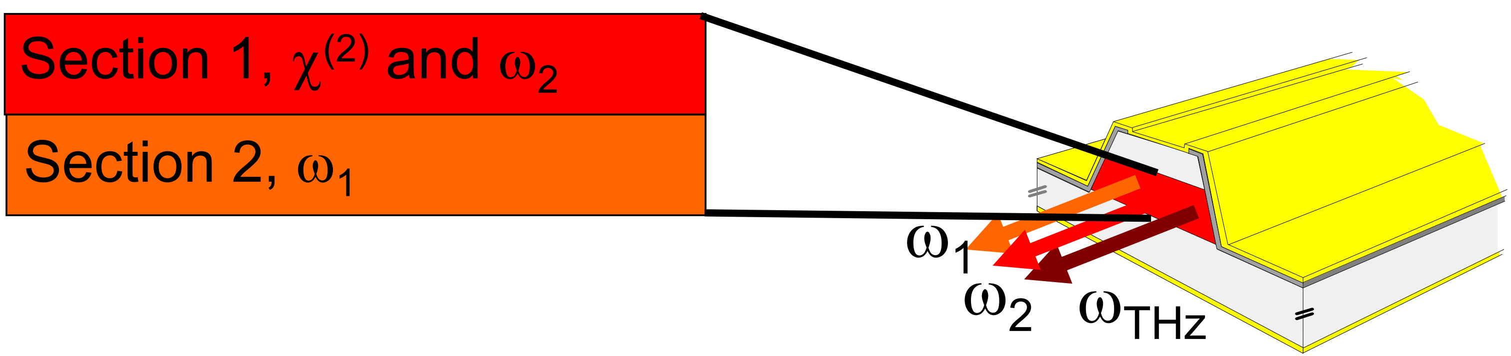

$\chi^{(2)}$-section design

Bound-to-continuum active region for $\lambda \approx 9\mu m$

[Faist et al. IEEE JQE (2002)]

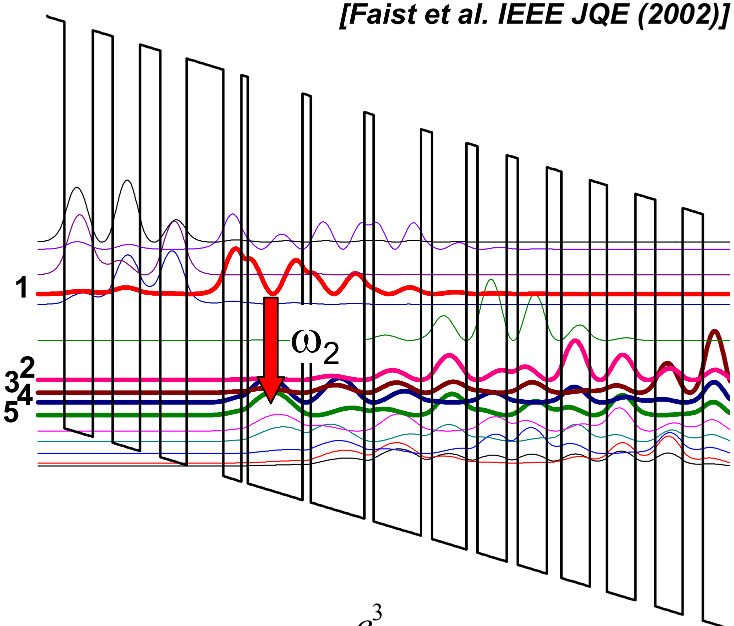

$$\chi^{(2)}(\omega=\omega_1-\omega_2)\approx N_e\frac{e^3}{\hbar^2\varepsilon_0}\times$$

$$\sum_{n,n'}\frac{z_{1n}z_{nn'}z_{n'1}}{(\omega-\omega_{nn'}+i\Gamma_{nn'})}\left(\frac{1}{(\omega_1+\omega_{n'1}+i\Gamma_{n'1})}+\frac{1}{(-\omega_2-\omega_{n1}+i\Gamma_{n1})}\right)$$

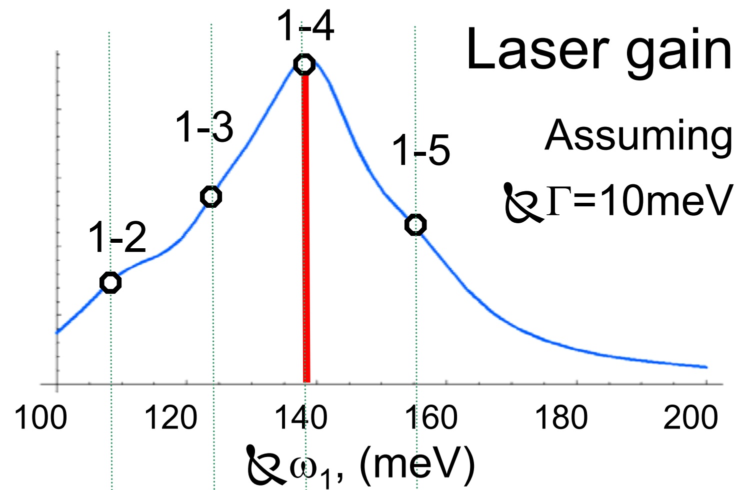

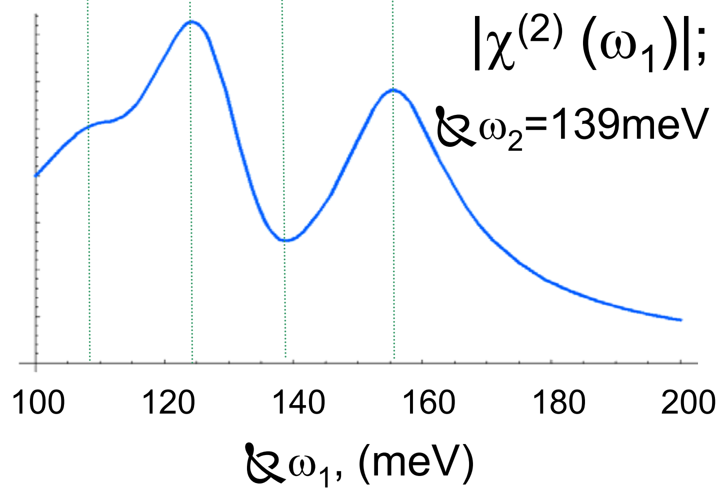

$\chi^{(2)}$-section design

Bound-to-continuum active region for $\lambda \approx 9\mu m$

[Faist et al. IEEE JQE (2002)]

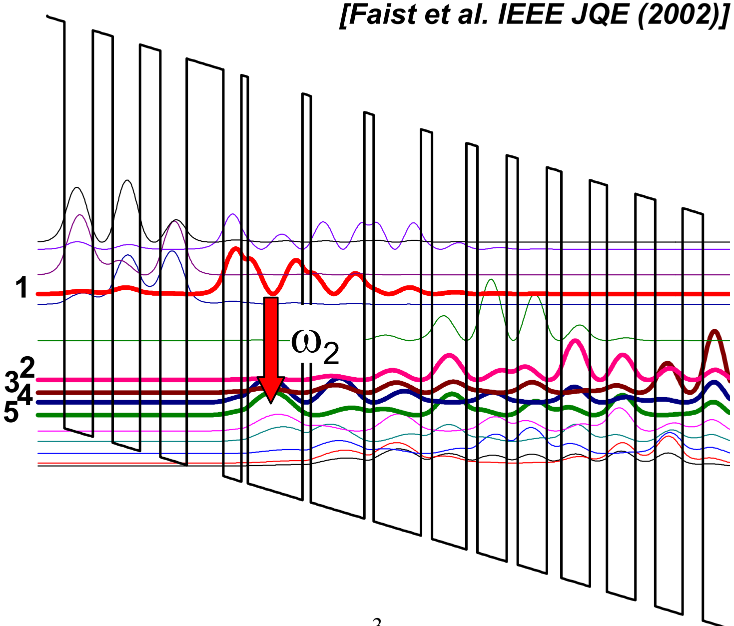

$$\chi^{(2)}(\omega = \omega_1 - \omega_2) \approx N_e \frac{e^3}{\hbar^2 \varepsilon_0} \times$$

$$\sum_{n,n'} \frac{z_{1n} z_{nn'} z_{n'1}}{(\omega - \omega_{nn'} + i\Gamma_{nn'})} \left(\frac{1}{(\omega_1 + \omega_{n'1} + i\Gamma_{n'1})} + \frac{1}{(-\omega_2 - \omega_{n1} + i\Gamma_{n1})} \right)$$

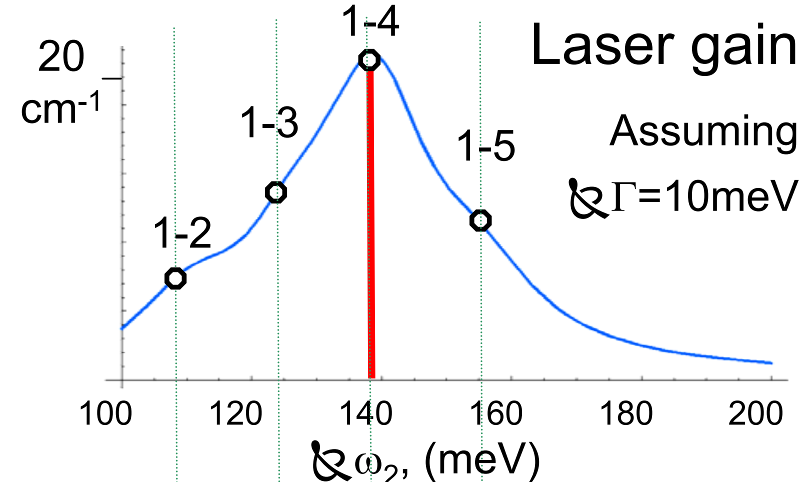

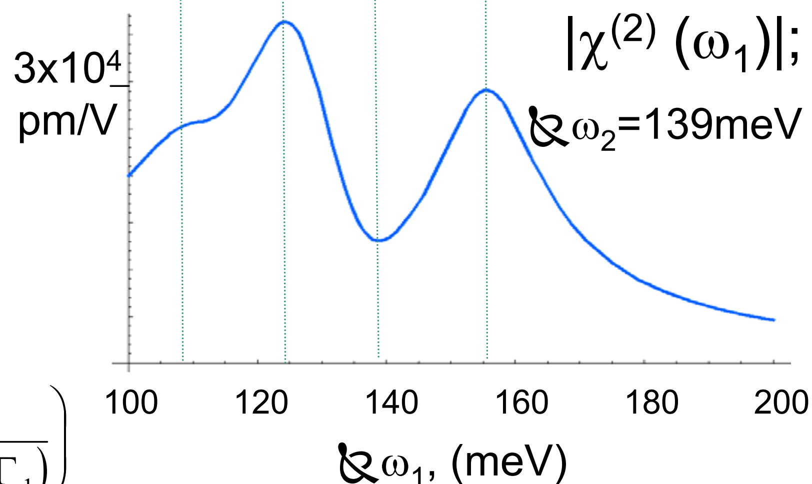

Active region design

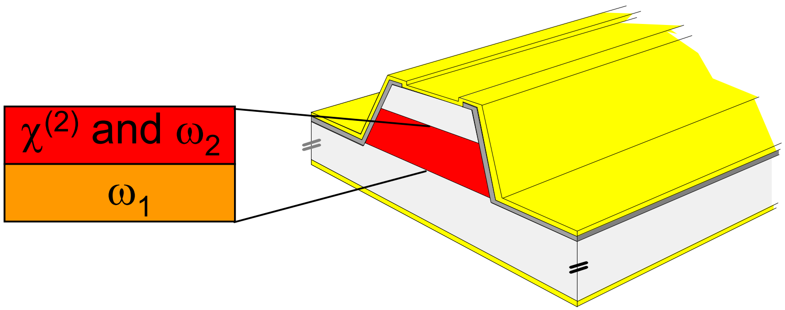

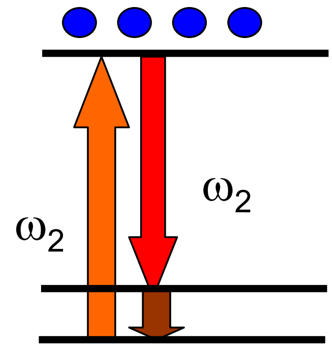

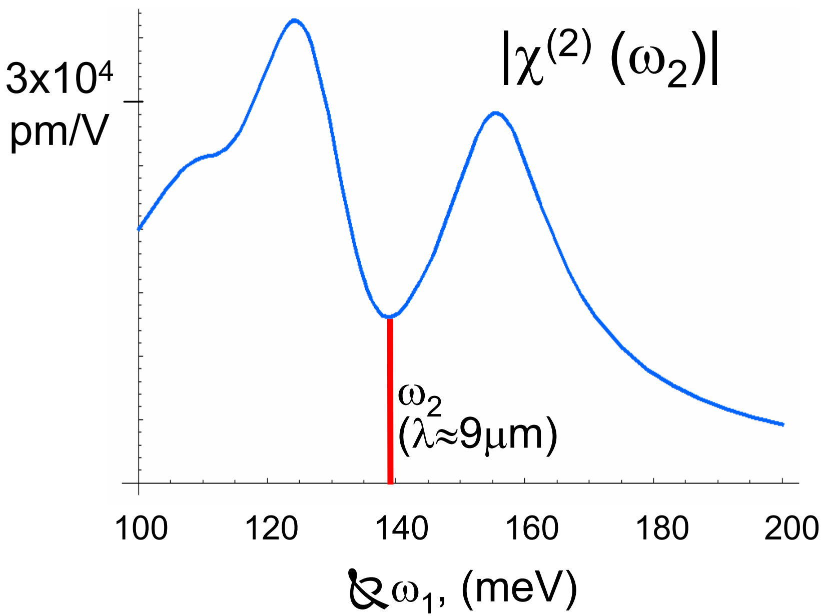

Section with ω_1 :

Active region design

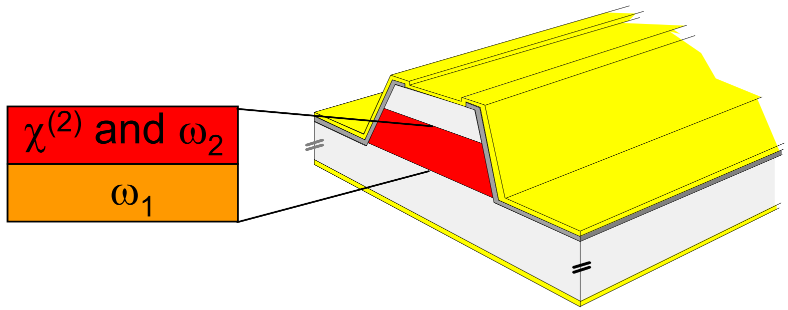

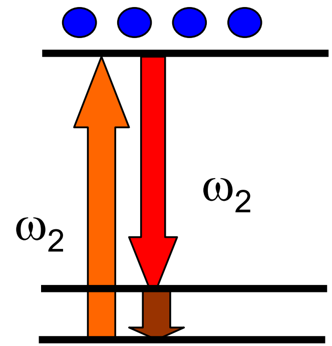

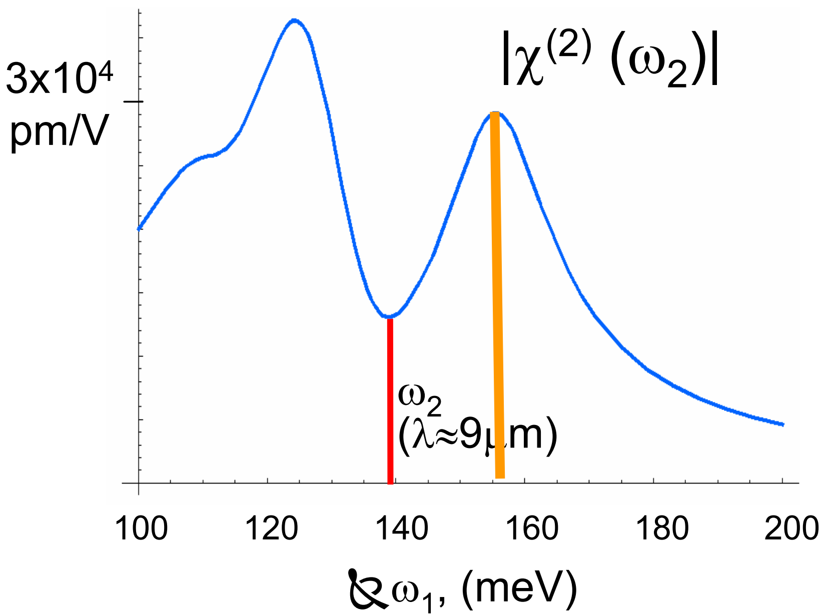

Section with ω_1 :

1. Two-phonon design at 155meV ($\lambda\approx 8\mu$m)

[Nature Photonics **1,** 288 (2007)]

Active region design

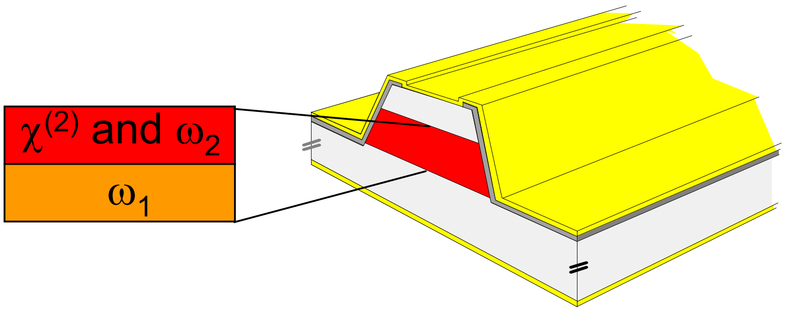

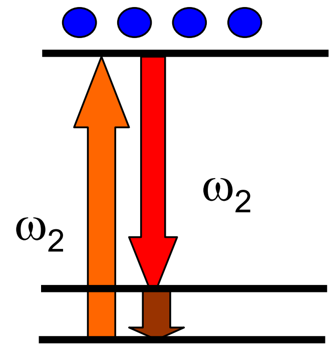

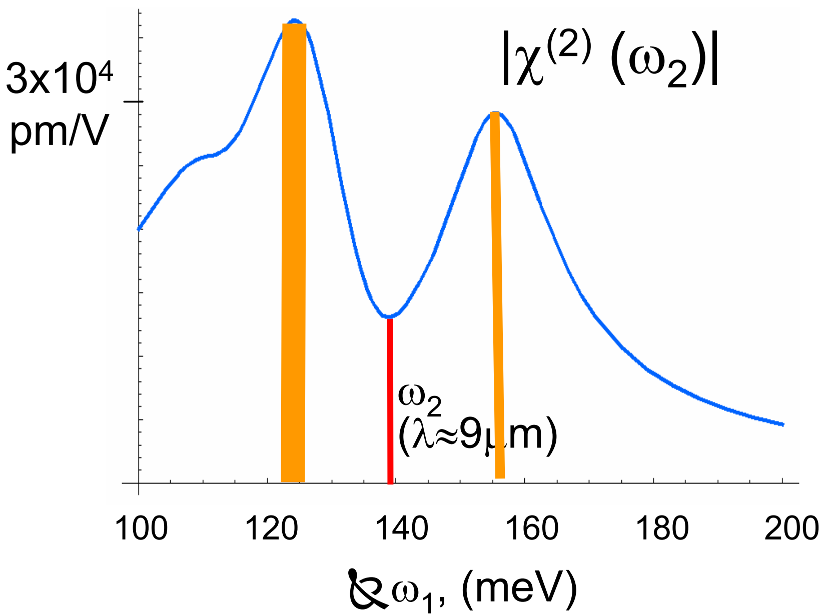

Section with ω_1 :

1. Two-phonon design at 155meV ($\lambda\approx8\mu$m)

[Nature Photonics **1**, 288 (2007)]

2. Two-phonon design at 125meV ($\lambda\approx10\mu$m)

Active region design

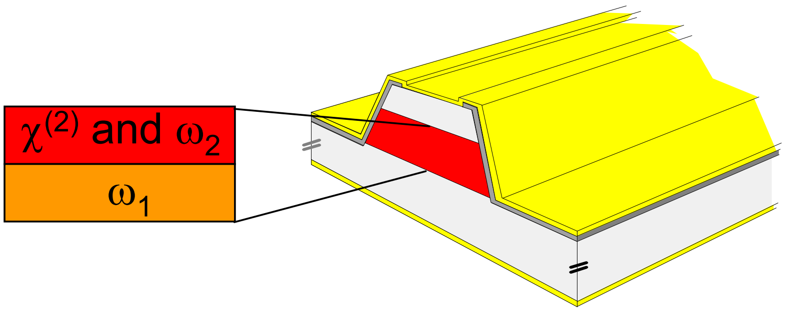

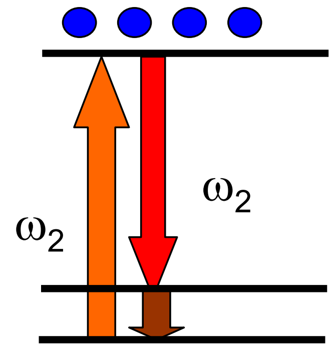

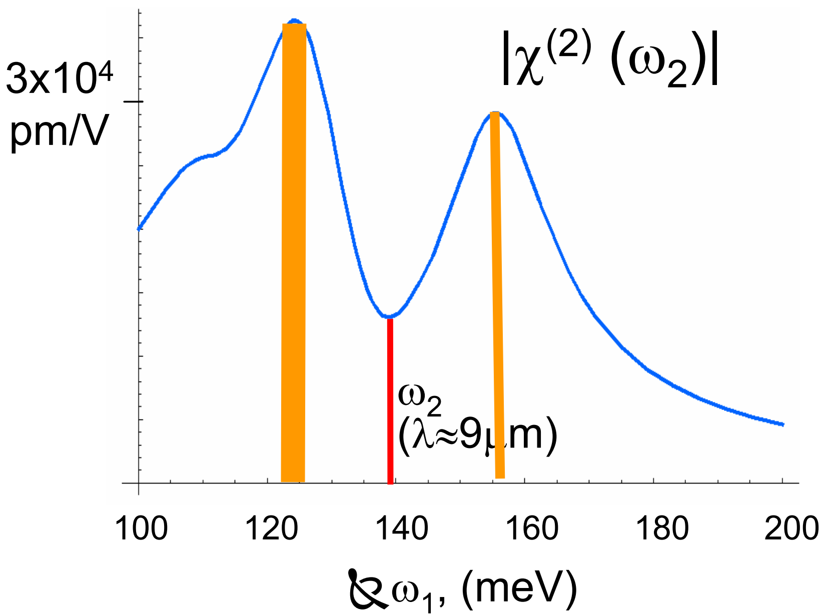

Section with ω_1 :

1. Two-phonon design at 155meV ($\lambda\approx 8\mu$m)

[Nature Photonics **1**, 288 (2007)]

2. Two-phonon design at 125meV ($\lambda\approx 10\mu$m)

Waveguide design

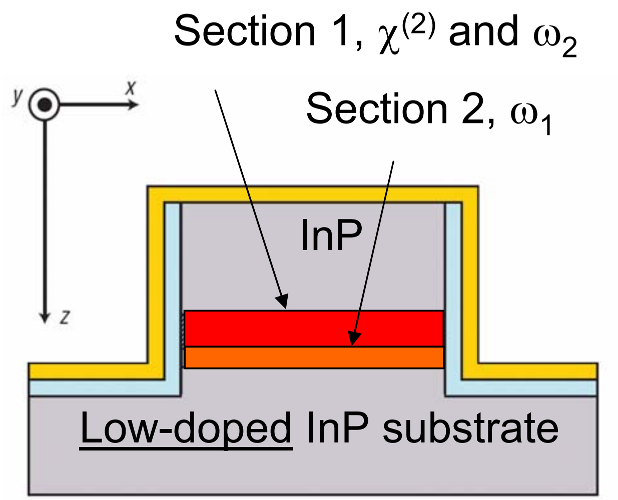

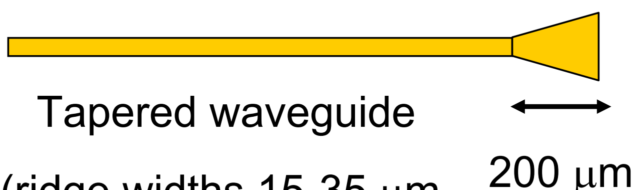

Tapered waveguide

(ridge widths 15-35 μm, tapered to 50 μm)

- *Dielectric waveguide for mid-IR modes*
- *Surface plasmon waveguide for THz mode*
- *Good THz out-coupling*
- *Close to phase matching due to Reststrahlenband*
- *l_{eff}≈70μm for DFG*

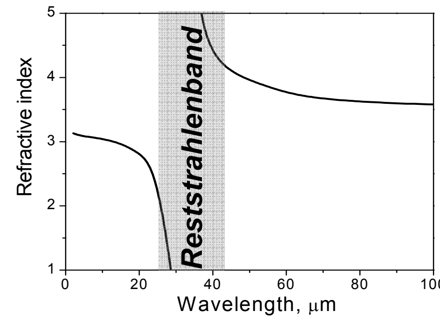

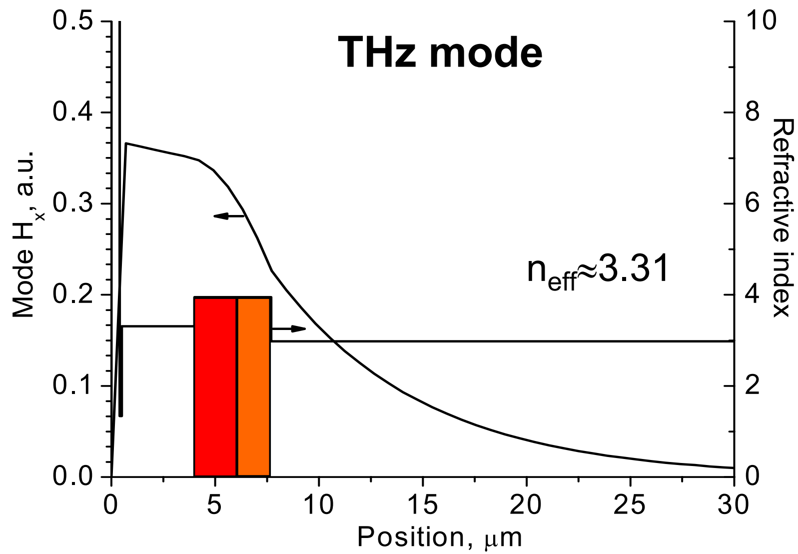

Device performance: mid-IR

Spectra

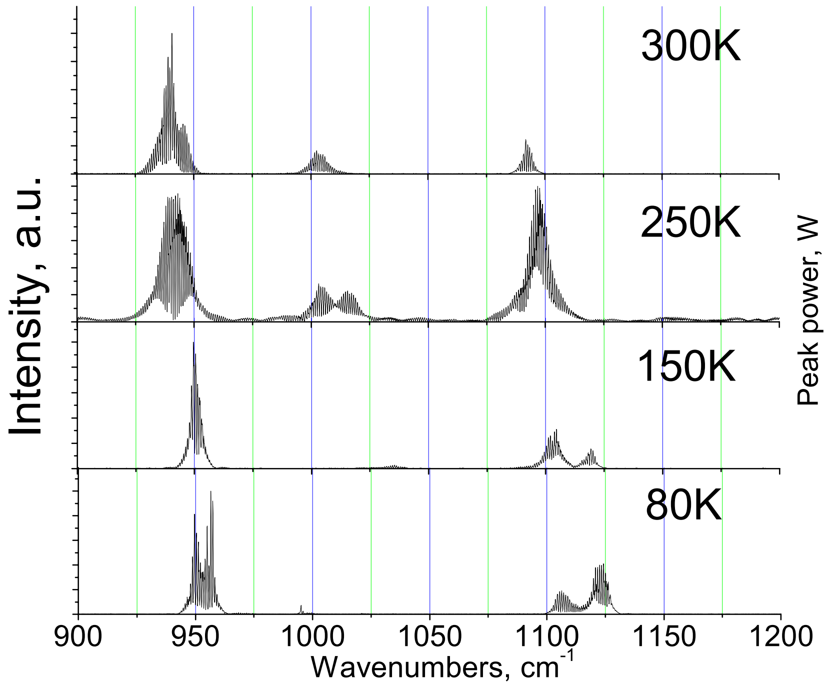

Power (combined)

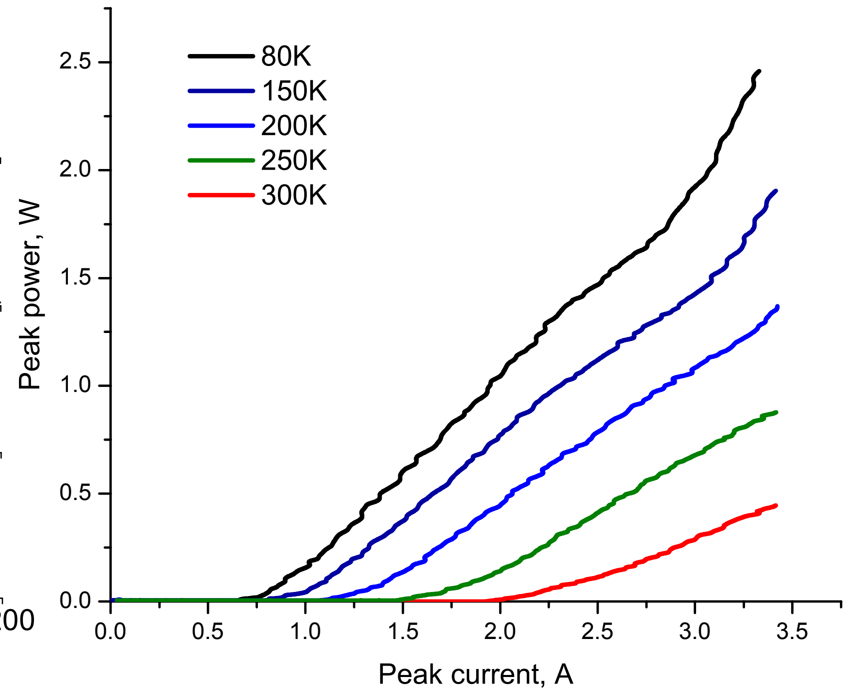

25-µm-wide, tapered to 50-µm-wide, 2-mm-long, back facet HR coating.
Testing in pulsed mode (60ns pulses at 250kHz).

Device performance: mid-IR

Spectra

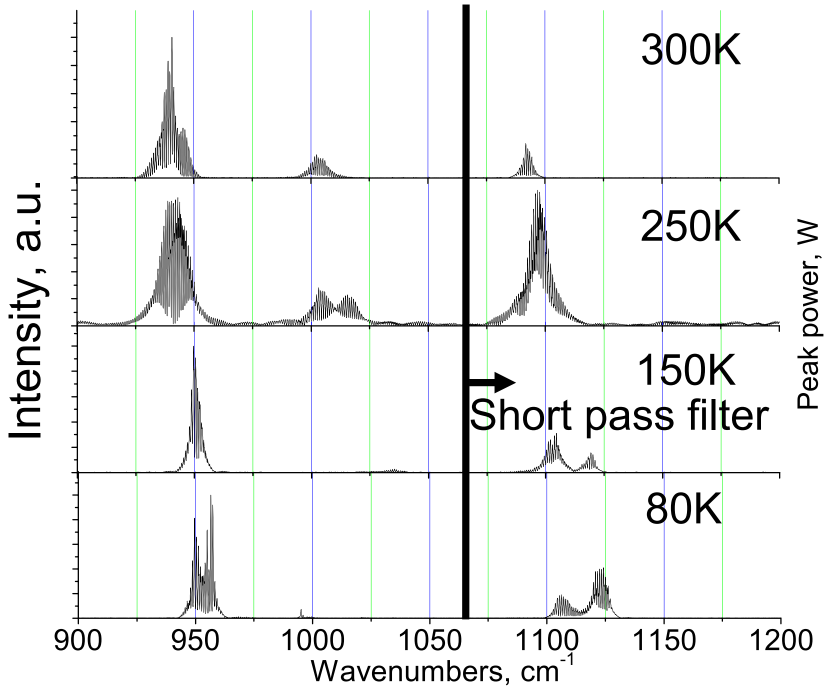

Power (combined)

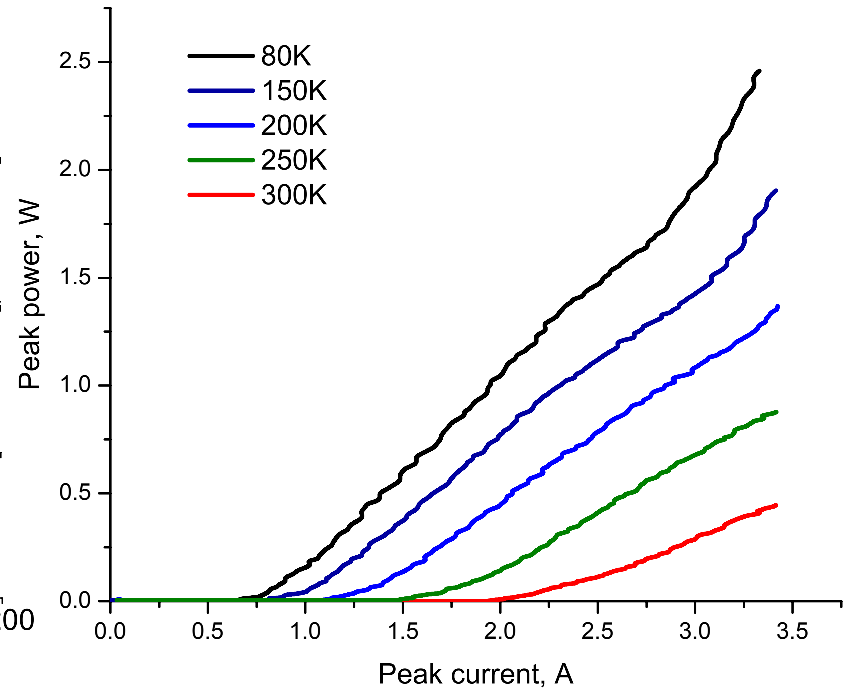

25-µm-wide, tapered to 50-µm-wide, 2-mm-long, back facet HR coating.
Testing in pulsed mode (60ns pulses at 250kHz).

Product of the pump powers

$$W(\omega_{THz}) \propto \left|\chi^{(2)}\right|^2 W(\omega_1) W(\omega_2) \times l_{eff}^2$$

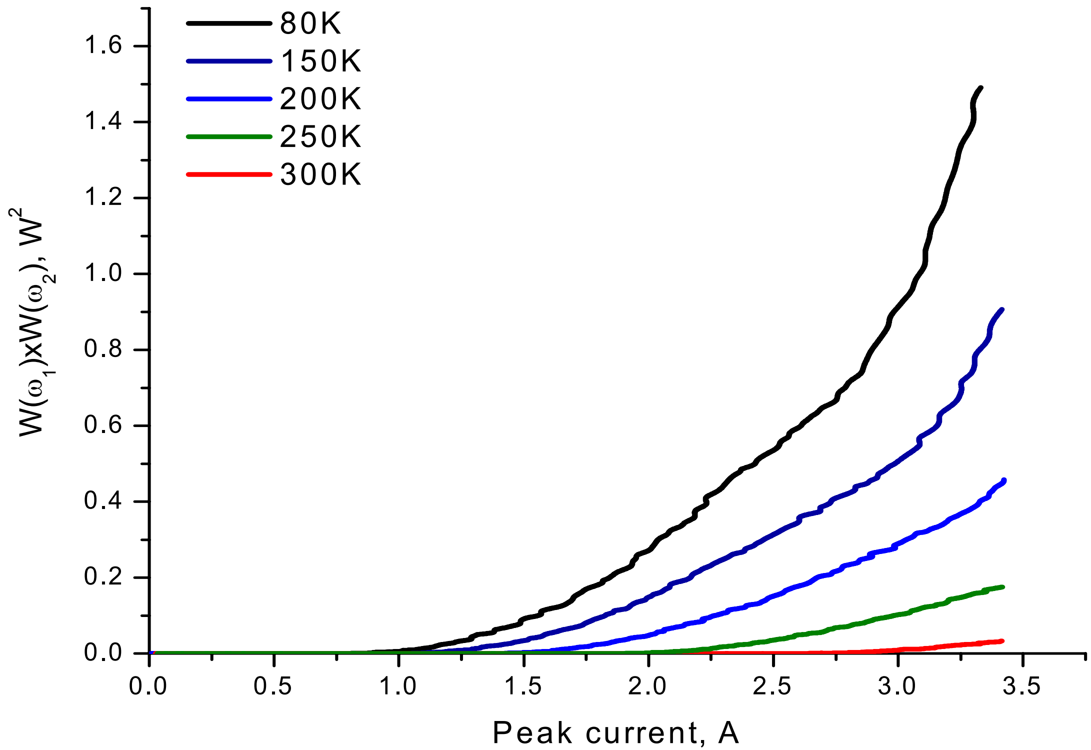

25-μm-wide, tapered to 50-μm-wide, 2-mm-long, back facet HR coating.
Testing in pulsed mode (60ns pulses at 250kHz).

Terahertz emission 80K

~1.5 μW of peak THz power at λ~65 μm

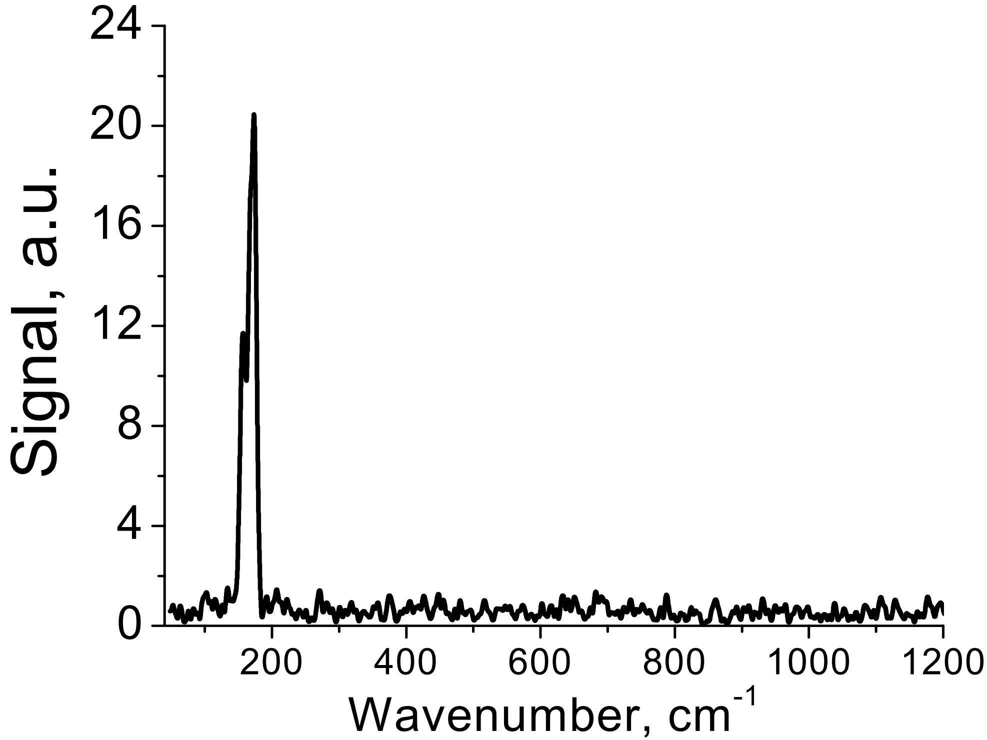

25-μm-wide, tapered to 50-μm-wide, 2-mm-long, back facet HR coating.
Testing in pulsed mode (60ns pulses at 250kHz).

Terahertz emission 80K

~1.5 μW of peak THz power at λ~65 μm

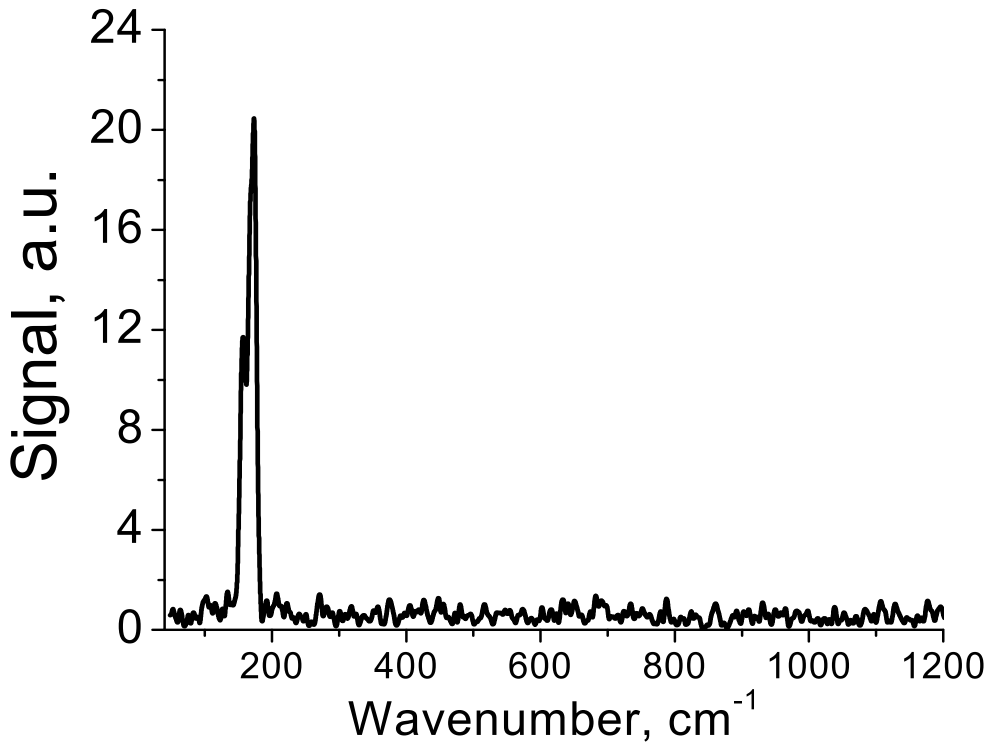

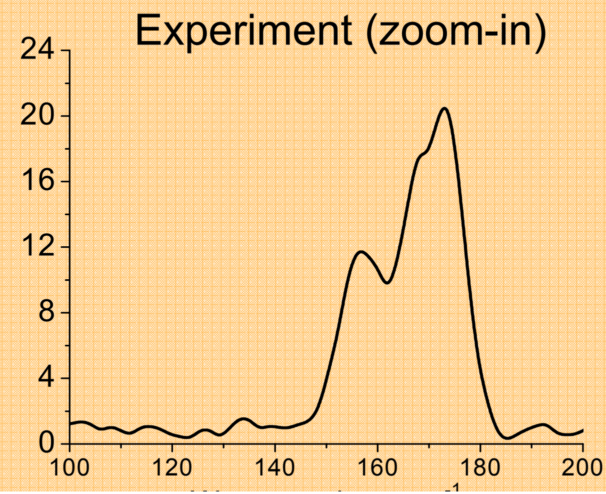

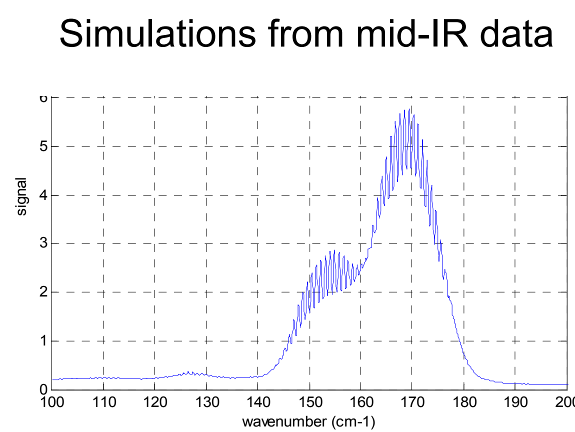

25-μm-wide, tapered to 50-μm-wide, 2-mm-long, back facet HR coating.
Testing in pulsed mode (60ns pulses at 250kHz).

Terahertz emission different T

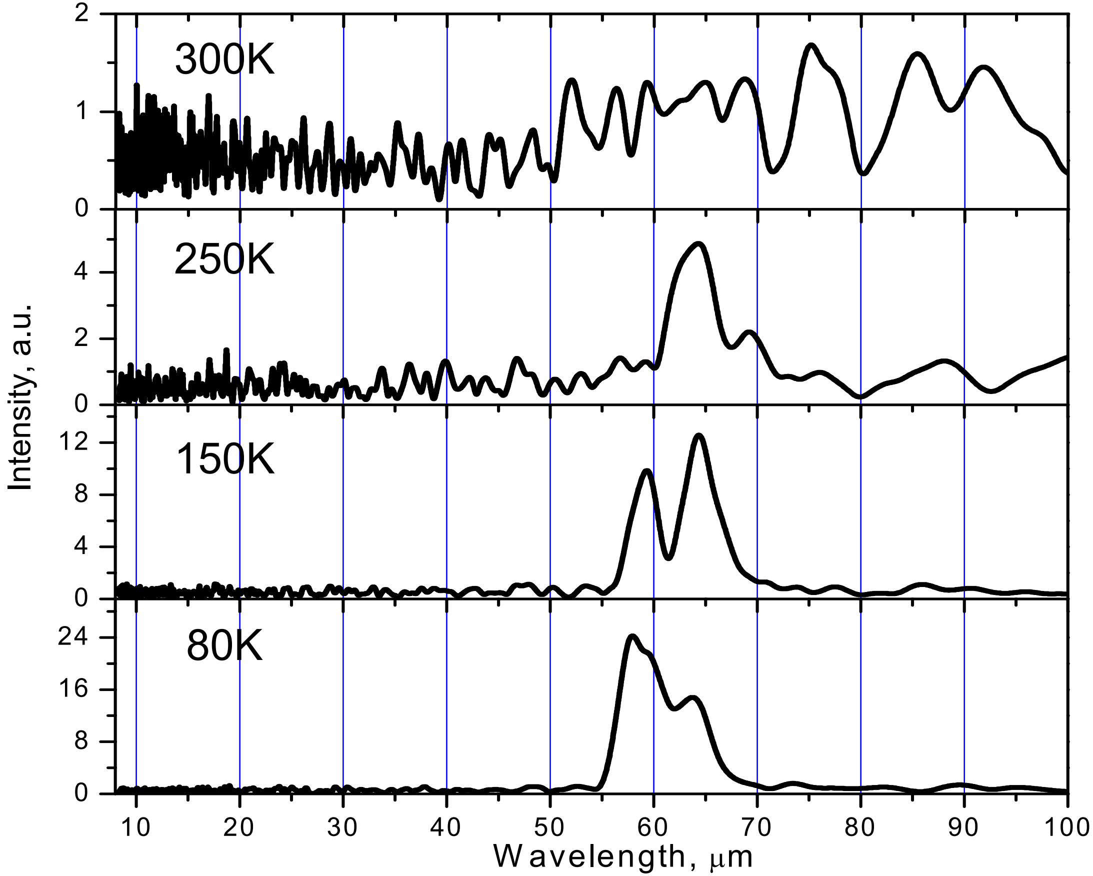

- Peak positions agree with mid-IR data
- Red-shift with temperature can also be observed in mid-IR data
- THz DFG signal observed up to 250K

25-μm-wide, tapered to 50-μm-wide, 2-mm-long, back facet HR coating.
Testing in pulsed mode (60ns pulses at 250kHz).

Terahertz emission

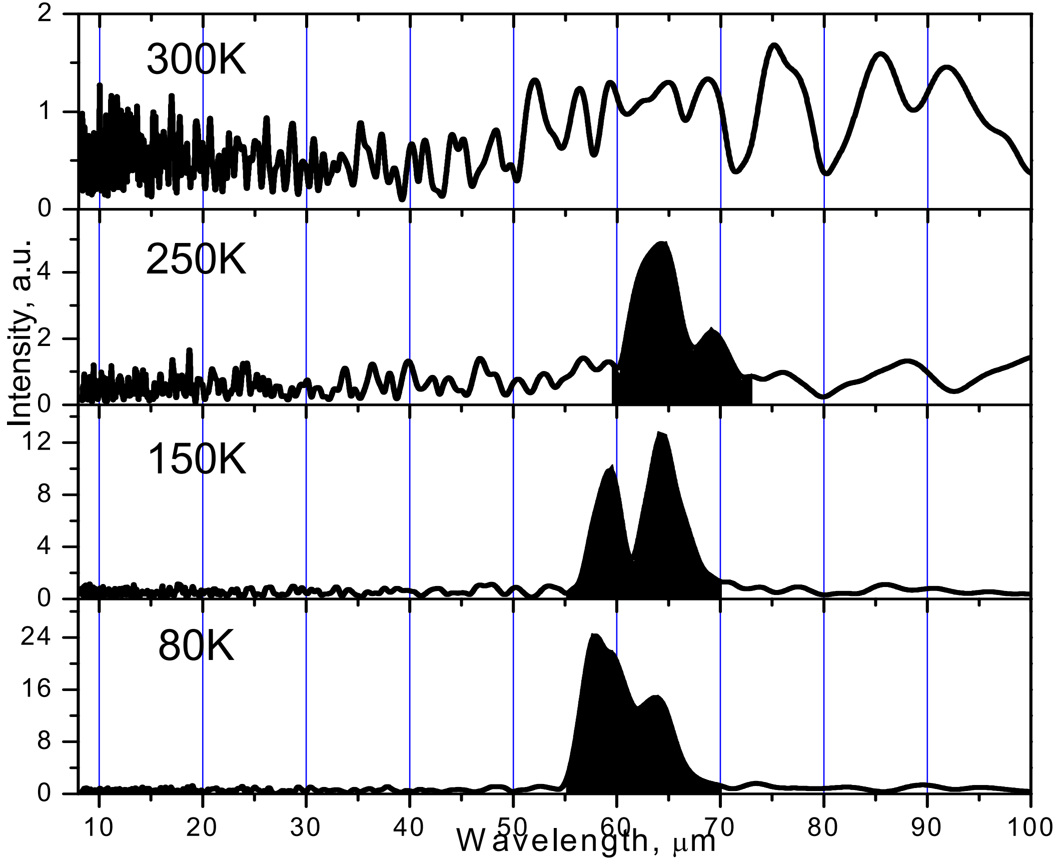

- Peak positions agree with mid-IR data
- Red-shift with temperature can also be observed in mid-IR data
- THz DFG signal observed up to 250K

25-μm-wide, tapered to 50-μm-wide, 2-mm-long, back facet HR coating.
Testing in pulsed mode (60ns pulses at 250kHz).

THz power/conversion efficiency

THz DFG power VS the product of mid-IR pumps powers at 80K

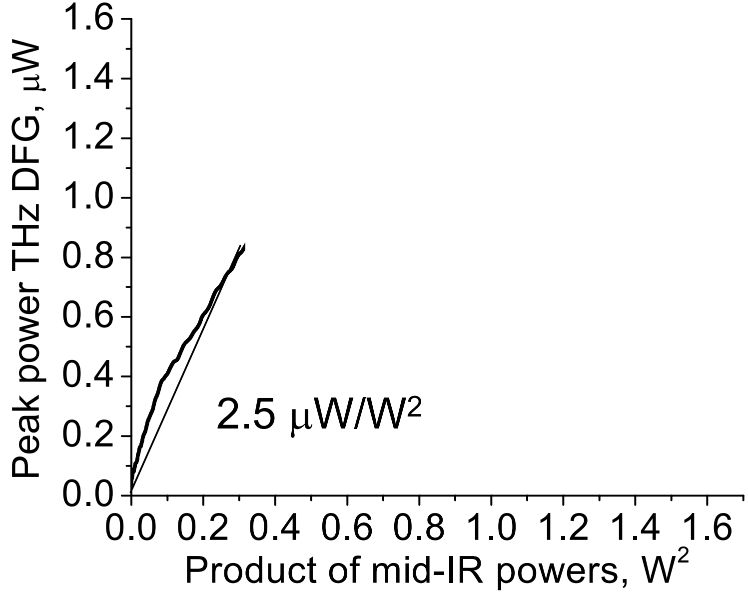

25-μm-wide, tapered to 50-μm-wide, 2-mm-long, back facet HR coating.
Testing in pulsed mode (60ns pulses at 250kHz).

THz power/conversion efficiency

THz DFG power VS the product of mid-IR pumps powers at 80K

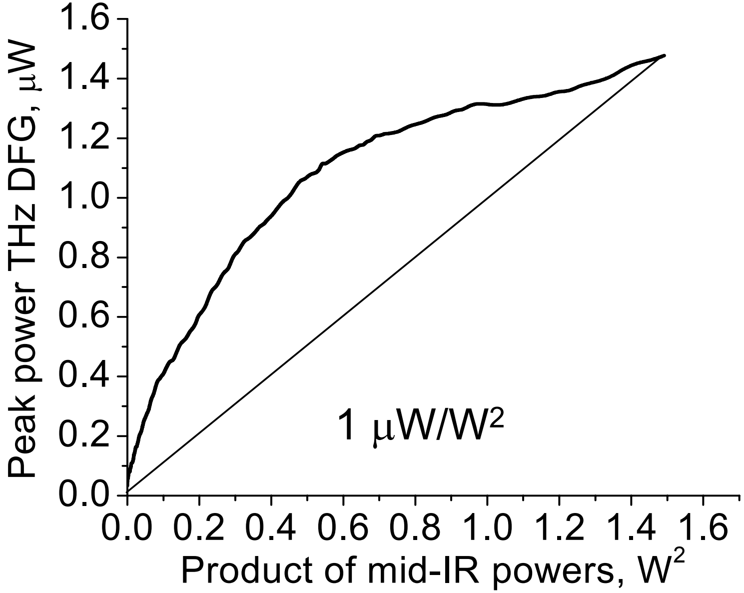

Conversion efficiency ~1μW/W^2

25-μm-wide, tapered to 50-μm-wide, 2-mm-long, back facet HR coating.
Testing in pulsed mode (60ns pulses at 250kHz).

THz power/conversion efficiency

THz DFG power VS the product of mid-IR pumps powers at 80K

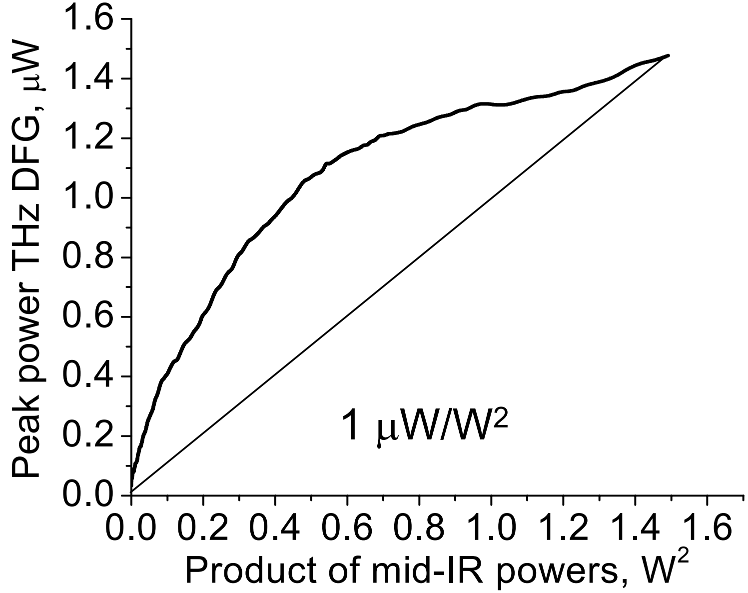

Peak THz DFG power and mid-IR power versus temperature

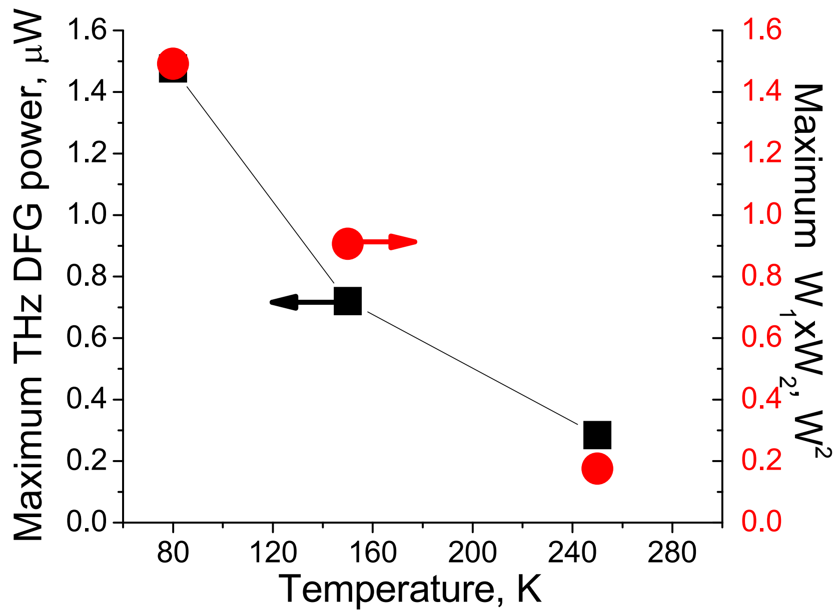

Conversion efficiency ~1μW/W²

THz DFG power scales with pump powers at high temepratures

25-μm-wide, tapered to 50-μm-wide, 2-mm-long, back facet HR coating.
Testing in pulsed mode (60ns pulses at 250kHz).

Conversion efficiency: analysis

$$W_{THz} \approx \frac{\omega^2}{8\varepsilon_0 c^3 n_{eff}^{\omega} n_{eff}^{\omega_1} n_{eff}^{\omega_2}} \times \frac{\left|\chi^{(2)}\right|^2}{S_{eff}} W_1 W_2 \times l_{eff}^2$$

S_{eff}, l_{eff}, refractive indices are known from waveguide calculations:

$n_{eff} \approx 3$, $l_{eff} \approx 90\ \mu m$, $S_{eff} \approx 1800\ \mu m^2$

Estimate $\chi^{(2)}$ using electron density in upper laser state from gain=loss condition:

$\chi^{(2)} \approx 4x10^4$ pm/V

Uncertain parameters:

Mid-IR lasing in higher order lateral modes

THz wave out-coupling efficiency from QCL waveguide (~10%?)

Conversion efficiency: analysis

$$W_{THz} \approx \frac{\omega^2}{8\varepsilon_0 c^3 n_{eff}^{\omega} n_{eff}^{\omega_1} n_{eff}^{\omega_2}} \times \frac{\left|\chi^{(2)}\right|^2}{S_{eff}} W_1 W_2 \times l_{eff}^2$$

S_{eff}, l_{eff}, refractive indices are known from waveguide calculations:

$n_{eff} \approx 3$, $l_{eff} \approx 90\ \mu m$, $S_{eff} \approx 1800\ \mu m^2$

Estimate $\chi^{(2)}$ using electron density in upper laser state from gain=loss condition:

$\chi^{(2)} \approx 4\text{x}10^4$ pm/V

Uncertain parameters:

Mid-IR lasing in higher order lateral modes

THz wave out-coupling efficiency from QCL waveguide (~10%?)

Theoretical efficiency: $W_{THz}/(W_1 \times W_2)$ ~ 10 μW/W^2

Experiment (corrected for the collection efficiency): ~ 1 μW/W^2

~10 times discrepancy

Future work

- *Attempt phase matching by varying waveguide width*
- *Improve edge emission out-coupling*
- *Surface emission scheme*
- *Novel active region designs*

Summary

- *Improved temperature performance and power of THz DFG in QCLs*
- *THz signal level is >1μW at 80K and still ~200nW at 250K*
- *Conversion efficiency is ~1 $\mu W/W^2$.*
- *Large room for conversion efficiency improvements*

Funding: AFOSR

The structures were processed in the Center for Nanoscale Science (CNS) in Harvard University.

Surface emission scheme

- *Only THz radiation generated within l_{eff} of the laser facet comes out of the device.*
- *Typical l_{eff}~100μm; QCL length ~3mm*
- *Laser ridge height and width are smaller than THz wavelength $\Rightarrow$ poor THz out-coupling*

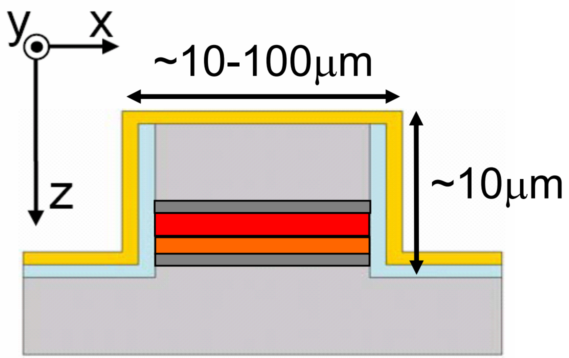

Surface emission

- Allows THz extraction along the whole device.
- Good THz beam quality.
- Out-coupling up to 30 cm^{-1}